New Journal of Physics
The open access journal at the forefront of physics
Deutsche Physikalische Gesellschaft DPG | IOP Institute of Physics

Paramagnetic dust particles in rf-plasmas with weak external magnetic fields

Marian Puttscher and André Melzer
Institut für Physik, Ernst-Moritz-Arndt-Universität Greifswald, 17487 Greifswald, Germany
E-mail: puttscher@physik.uni-greifswald.de and melzer@physik.uni-greifswald.de

Received 28 December 2013, revised 12 March 2014
Accepted for publication 24 March 2014
Published 29 April 2014
New Journal of Physics **16** (2014) 043026
doi:10.1088/1367-2630/16/4/043026

Abstract
Experimental studies on dusty plasmas containing systems of (super-)paramagnetic dust particles are presented. In our experiments, external (homogeneous as well as inhomogeneous) magnetic fields in the mT range are applied to study the effect on single particles or few-particle systems that are trapped inside the sheath region. The behavior of the paramagnetic dust particles is considerably different than that of dielectric plastic particles, which are widely used in dusty plasmas. It is revealed that especially non-magnetic contributions play an important role in the interaction between superparamagnetic particles.

Keywords: dusty plasmas, paramagnetic particles, magnetic fields

1. Introduction

Nanometer-sized to micrometer-sized particles in dusty (complex) plasmas attain a high negative charge by the collection of electrons and ions. Then, the electrostatic interaction can typically be described by a screened Coulomb (Yukawa) interaction. In contrast, interactions with magnetic fields have been much less explored for dusty plasmas. Electrostatically interacting dust particles have been studied with respect to crystallization, charging or waves (see [1–7]).

The presence of external magnetic fields is of importance for plasmas, not only in fusion research. For example, magnetic fields are also used in magnetically enhanced reactive ion

Content from this work may be used under the terms of the Creative Commons Attribution 3.0 licence. Any further distribution of this work must maintain attribution to the author(s) and the title of the work, journal citation and DOI.

© 2014 IOP Publishing Ltd and Deutsche Physikalische Gesellschaft

etching reactors as well as in magnetron sputtering devices; see [8, 9]. Transverse magnetic fields even in the mT range have been shown to influence plasma properties like, e.g., the electron density. This is reported in, e.g., [8, 10, 11] for a wider range of magnetic field strength for neutral gas pressures comparable to ours. [8, 12] examined the structure of an rf discharge under the influence of a transverse magnetic field, showing that the maximum excitation and plasma production occur closer to the powered electrode as the magnetic field strength increases. Hence, it is also interesting to study magnetic field effects in dusty plasmas.

Normally, for colloidal plasmas, experiments are performed with dielectric plastic spheres and a commonly used particle material is melamine formaldehyde (MF). In this work we investigate two-dimensional dust clouds consisting of (super)paramagnetic particles under weak external magnetic fields. Dusty plasma systems with paramagnetic particles have been studied relatively rarely, so far. Samsonov *et al* [13] reported on the enhanced levitation of whole dust clouds by an inhomogeneous magnetic field with gradients of up to 5 T/m. The ground state structure of two-dimensional particle layers with a magnetic dipole–dipole interaction between the dust particles competing with the Yukawa interaction is described by simulations in [14, 15]. Axial magnetic fields were applied to dusty plasmas with non-magnetic spheres in, e.g., [16–19]. There it has been reported that dust clusters were set into rotation due to the interaction of the magnetic field with ions and neutrals. An $\vec{E} \times \vec{B}$-induced ion flow sets the neutral gas into rotation, which in turn affects the dust particles.

In this work, dusty plasmas with paramagnetic particles are studied experimentally. An external (homogeneous as well as inhomogeneous) magnetic field in the mT regime is applied horizontally and the influence on the particle system is studied. Comparative measurements with MF particles were also performed. We will specifically also address non-magnetic contributions to the particle interaction.

2. The experiment

Our experiments were performed in a capacitive argon rf discharge at neutral gas pressures of the order of 1 to 10 Pa. The lower aluminum electrode is driven at 13.56 MHz. The discharge vessel and the upper electrode (both also made of aluminum) are grounded. The particles are trapped in the sheath of the discharge by a balance of gravitational and electric field force. For radial confinement, the driven electrode is provided with a shallow trough. The total potential energy of the dust cluster in the horizontal plane is then given by a combination of the radial confinement potential and the Yukawa interaction:

$$E_{pot} = \frac{1}{2} m_d \omega_0^2 \sum_{i=1}^{N} r_i^2 + \frac{Q_d^2}{4\pi\epsilon_0} \sum_{i<j}^{N} \frac{\exp\left(-r_{i,j}/\lambda_D\right)}{r_{ij}}. \quad (1)$$

Here, m_d is the mass of a dust particle, ω_0 is a measure of the trapping strength and r_i is the radial displacement from the center. Q_d, ϵ_0, λ_D and r_{ij} are the electrical charge of the particles, permittivity of vacuum, Debye length and interparticle distance of particles i and j, respectively.

The particles are illuminated with a laser and the scattered light is detected by fast video cameras (frame rate: about 100 frames s^{-1}) to track the particle motion. Experiments in this work were performed with either 664 nm (red) or a 532 nm (green) laser illumination. If not stated otherwise, the 532 nm laser was used to illuminate the particle clusters.

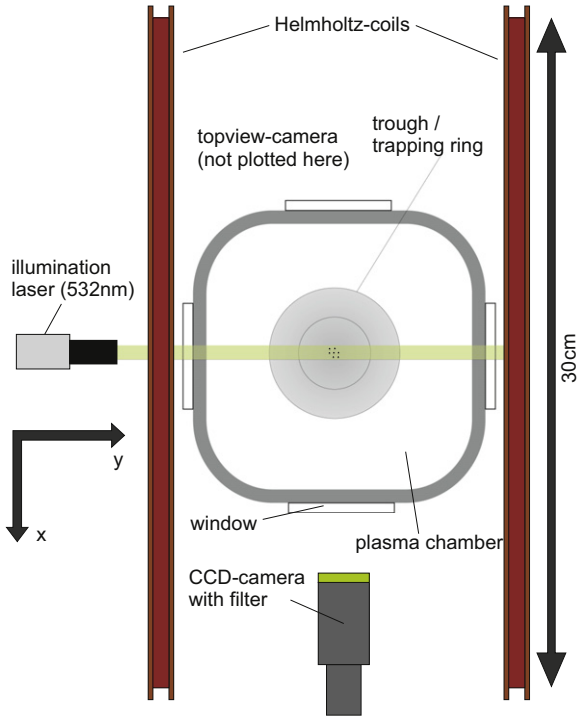

Figure 1. Experimental setup in a top view.

The magnetic field is produced by upright (Helmholtz) coils. Thus, in the volume where the particles are captured, the magnetic field lines are parallel to the electrode surface. In figure 1 a schematic top view drawing is shown. To account for the influence of the orientation of the magnetic field, the magnetic field coils could also easily be oriented parallel to the electrodes, producing an axial field. The coils are made of enameled copper wire and the maximum current through the coils is 2 A. Hence, using both coils in a Helmholtz arrangement, the maximum field strength in the center is

$$B_{HH} = \sqrt{\frac{64}{125}}\frac{\mu_0 NI}{R} \approx 1.15\ \text{mT} \tag{2}$$

which was also verified using a gaussmeter. Here, μ_0 is the magnetic permeability of vacuum, $N = 94$ is the number of windings and $I = 2$ A is the electrical current through the coils. The radius R of the coils is roughly 15 cm.

In order to perform investigations on particles in inhomogeneous fields, only one coil was driven. The magnetic field on the axis of symmetry for a single coil and at the location of the particles at a distance of $R/2$ from the coil is then $B_1 = 0.57$ mT and its gradient at the position of the particles is

$$\nabla B_1 = \frac{6B_1}{5R} = 4.6\ \text{mT/m}, \tag{3}$$

which agrees well with a measured value of 5.3 mT/m.

In our experiments we used paramagnetic spherical polystyrene particles with diameters of 4 and 9 μm which are paramagnetic due to homogeneously incorporated nanoscale iron oxide [20].

These particles have a saturation magnetic moment per mass of approximately 20 A m^2 kg^{-1}, and thus the maximum magnetization is of the order of $M_{sat} \approx 1.5 \times 10^{-12}$ A m^2 for the 4 μm particles and $M_{sat} \approx 1.4 \times 10^{-11}$ A m^2 for the 9 μm particles. Because of their low residual magnetism, in the range of $M_r = 0.01$ to 0.1 A m^2 kg^{-1}, they are nearly superparamagnetic. For comparative measurements, dielectric, non-magnetic MF particles with a diameter of 12.26 μm were also used.

3. Results and discussion

In this section, experiments with the paramagnetic particles are described and observations are discussed. The experimental findings are compared to those obtained using standard MF particles. We start with measurements on a single particle.

3.1. Single dust particles

In this section, experiments on only one particle trapped in the discharge are described and the movement of this single paramagnetic dust particle in the presence of an externally applied magnetic field is studied. The gas pressure was 10 Pa, here. The illumination laser was not driven continuously, but pulsed, and the particle positions were calculated from those images where the laser was just turned on. After this illumination pulse the laser was switched off for several seconds to guarantee non-disturbed dust particle motion at the next illumination flash. The reason for this practice will be given in section 3.3.

Figure 2 shows the dependence of the displacement of the 4 μm diameter particle perpendicular (x-direction) and parallel (y-direction) to the magnetic field on the field strength B. The particle motion is measured both for a homogeneous and for an inhomogeneous field. For clarity, the directions of $\vec{B}$, $\nabla\vec{B}$ and $\vec{E} \times \vec{B}$ are also given in the figures. First, we consider the movement perpendicular to the magnetic field; see figure 2(a). The figure shows that the dust particles are pushed in the $-\vec{E} \times \vec{B}$ direction, where $\vec{E}$ is the vertical electric field in the plasma sheath. To explain this behavior we follow the idea of an ambipolar $\vec{E} \times \vec{B}$-drift presented in [21]. For our experimental parameters, only the electrons are magnetized; the ions and dust particles are not. Since the electrons are able to execute the $\vec{E} \times \vec{B}$-drift, a space charge electric field develops, between the drifting electrons and the heavier non-magnetized ions. The non-magnetized and negatively charged dust particles embedded into this ambipolar electric field move towards the positive pole. Thus, they are drifting in the direction opposite to the electron drift, namely in the direction of $-\vec{E} \times \vec{B}$. A larger displacement at increasing magnetic field qualitatively agrees with [21]. As mentioned in section 2, a shallow trough was placed onto the driven electrode; thus the dust particles could not escape horizontally, but settled into a new equilibrium position. In this steady state the trapping force cancels the $\vec{E} \times \vec{B}$ ambipolar force, which arises from the ambipolar field and acts on the dust particles. Assuming a harmonic horizontal confinement, the force balance is

$$m_d \omega_0^2 \Delta x = Q_d E_{amb}. \tag{4}$$

Here, Δx is the displacement from the center perpendicular to the magnetic field and $\omega_0/2\pi \approx 1/s$ is the strength of the horizontal confinement due to the trough, as computed from

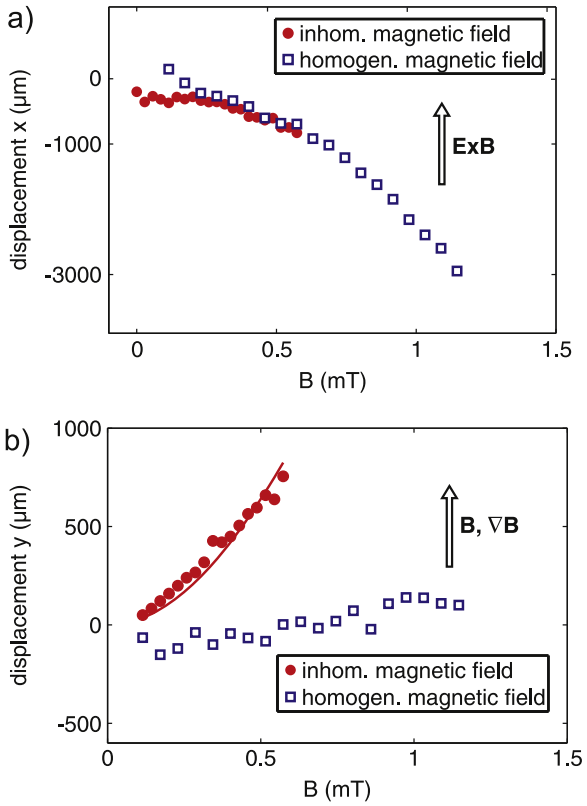

Figure 2. Displacement of a single superparamagnetic particle perpendicular (a) and parallel (b) to the magnetic field. Here, both homogeneous and inhomogeneous magnetic fields have been applied. In (a) an ambipolar $\vec{E} \times \vec{B}$-drift causes the dust particle to move in the direction opposite to $\vec{E} \times \vec{B}$. This is superposed by a movement towards the stronger magnetic field (b). The solid line in (b) is a fit to equation (7).

the normal mode analysis; see section 3.4. Since the dust charge $Q_d \approx 8500$ elementary charges is also known from the normal mode analysis, equation (4) yields an ambipolar electric field of the order of 10 V/m, which is a small horizontal disturbance of the sheath electric field at the particle position.

Next, we discuss the particle movement along the direction of the magnetic field; see figure 2(b). For the homogeneous field it is seen that the particle is not displaced along the field direction, since $\nabla B \approx 0$. By using just one of the coils, an inhomogeneous magnetic field is applied to the plasma. Now, a force due to the field gradient pushes the particle towards the stronger magnetic field, i.e. towards the coil. So, in these experiments, we see a superposition of the perpendicular motion in the $-\vec{E} \times \vec{B}$-direction and the parallel displacement due to the force

$$\vec{F}_{\nabla B} = \vec{M}\, \nabla \vec{B}_1. \tag{5}$$

In equilibrium, F_{trap} and $F_{\nabla B}$ are equal, which gives one the opportunity to calculate the magnetic moment of the particles. First, the magnetic moment induced by the external field B is given by the Langevin equation

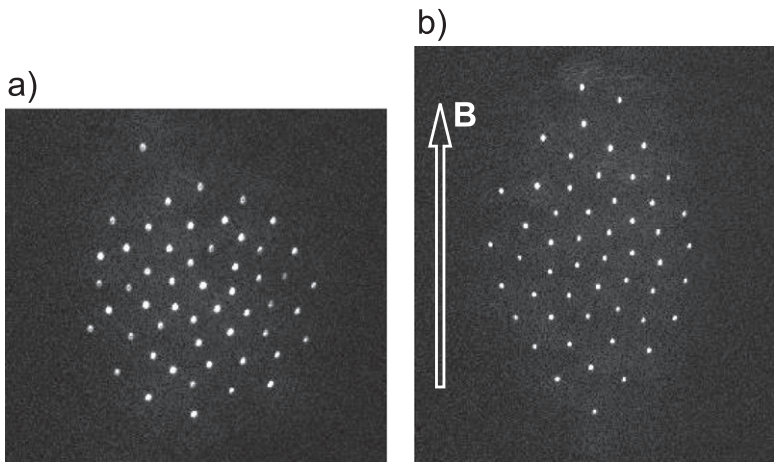

Figure 3. Top view camera snapshots of two-dimensional paramagnetic dust particle systems at a neutral gas pressure of 10 Pa. (a) Dust layer without external magnetic field, and (b) at maximum homogeneous magnetic field (≈1.15 mT).

$$M = M_0 \left[\coth\left(\frac{\mu B}{k_B T}\right) - \frac{k_B T}{\mu B} \right], \tag{6}$$

where μ is the magnetic moment of a single nanoscale iron oxide cluster inside the particle matrix, T is the iron oxide temperature and k_B is Boltzmann's constant. Now, equations (3), (6) and the force balance between F_{trap} and $F_{\nabla B}$ yield

$$\Delta y = \frac{6M_0}{5m_d\omega_0^2 R} \left[\coth\left(\frac{\mu B_1}{k_B T}\right) - \frac{k_B T}{\mu B_1} \right] B_1. \tag{7}$$

From a fit of the dependence of Δy on B_1 (the solid line in figure 2(b)), the factor $\mu/(k_B T)$ is obtained, and so the magnetic moment M can be calculated using equation (6). The magnetic moment obtained for the dust particle is about $M = 10^{-12}$ A m^2. This is thus reasonable, because $M_r \ll M \ll M_{sat}$, i.e., the measured value does not exceed the given saturation value and also exceeds the residual magnetism. It should be noted that even if the magnetic moments were saturated, the forces arising from the magnetic dipole–dipole interaction would be small compared to the Yukawa interaction; see the discussion in section 3.5.

3.2. Two-dimensional dust clouds

We now consider measurements on two-dimensional dust clouds of the superparamagnetic particles. For comparison, the same measurements have been performed with the standard MF particles (figures are not shown for MF). Without an external magnetic field, the shape of the dust cloud is circular, as expected from the radial confinement; see figures 3(a) and 4(a). The system is in a fluid state, as is implied by the trajectories in figure 4(a). This is in contrast to the case for MF particle systems, which are much more ordered at this neutral gas pressure of 10 Pa.

Now, the magnetic field is switched on; see figures 3(b) and 4(b). It is seen that the dust cluster is stretched along the direction of the magnetic field. MF systems do not show any significant change under the influence of this magnetic field. Hence, the stretching is not a

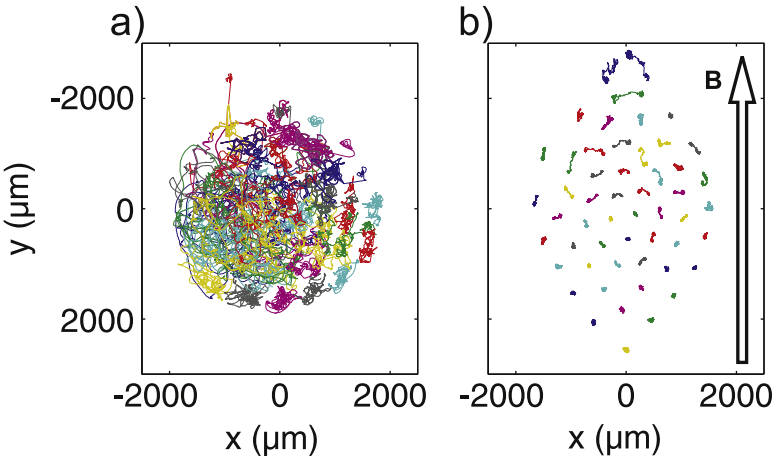

Figure 4. Trajectories of the dust particles, (a) without magnetic field and (b) with the maximum homogeneous magnetic field (1.15 mT) at a neutral gas pressure of 10 Pa.

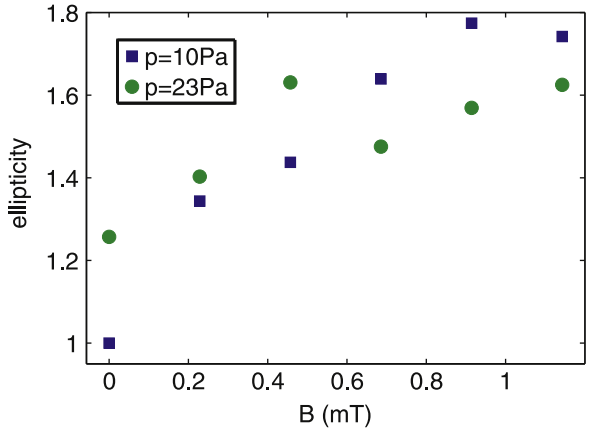

Figure 5. Dependence of the ellipticity of the dust clouds on the applied magnetic field.

plasma-related effect. We define the ellipticity as the ratio of major axis (along the field) divided by the minor axis (transverse to the field); see figure 3(b). The behavior of the ellipticity with increasing magnetic field is plotted in figure 5 for two different neutral gas pressures. The ellipticity becomes larger when the magnetic field strength is increased. In this parameter regime the ellipticity depends roughly linearly on the applied magnetic field and, for the maximum B-field in this experiment, the enlargement in the magnetic field direction is about 60% to 70% of its original dimension (for the case of p = 23 Pa, the ellipticity without a magnetic field is somewhat larger than unity due to the fact that at larger gas pressures the neutral gas drag from the steady gas flow affected the dust cloud.). This stretching of dust clusters is also found in inhomogeneous magnetic fields, i.e. when only one coil was used. For the Helmholtz arrangement (with two coils) the field inhomogeneity is weaker by orders of magnitude. So, the occurrence of this stretching does not depend on the grade of homogeneity of the magnetic field. Furthermore, if the magnetic dipole–dipole interaction were to be comparable to Yukawa interaction, the structure of the two-dimensional dust cluster would be expected to be different; see [14, 15]: depending on the relative orientation of the magnetic

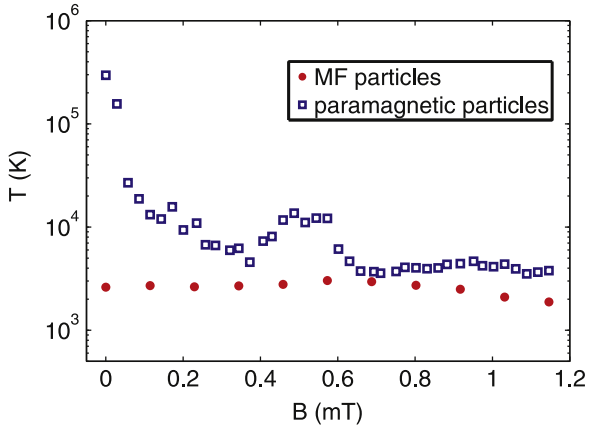

Figure 6. Dependence of the kinetic temperature of the paramagnetic and MF particles on the magnetic field strength.

moments, the magnetic dipole–dipole interaction is attractive or repulsive. This would lead to a 'striped' dust cloud, where particles form parallel chains that align along the magnetic field.

Further, as the magnetic field increases, particle motion becomes less violent; see figure 4(b). It is found that the kinetic temperature of the dust particles rapidly decreases with increasing field until a saturation at a lower temperature is reached and then remains approximately constant. In contrast, the temperature of the MF particles remains constant over the whole parameter regime from 0 to 1.15 mT. An example measurement of the particle temperature for p = 7.5 Pa (paramagnetic particles) and p = 3.8 Pa (MF particles) is shown in figure 6. The decreased temperature also becomes noticeable in the trajectories; see figure 4(b). At high field, the particles mainly perform small-scale oscillations around their equilibrium positions; the fast large-scale movement seen in the case without an applied magnetic field (see figure 4(a)) is gone. A lesser effect is observed at higher neutral gas pressures, explainable by greater damping. There the temperatures without magnetic field are smaller and so is the temperature difference compared to the case of maximum magnetic field. Note that in figure 6 even the MF particles have temperatures well above room temperature. While the particles are cooled by the neutral gas, additional heating might occur due to randomly fluctuating charge of the particles and fluctuating electric fields; see [22, 23] for details. At large magnetic fields, the temperatures of the paramagnetic particles and MF particles are of the same order.

We also performed measurements with the coils arranged parallel to the electrode (axial magnetic field). There, the trend to lower temperatures with increasing magnetic field could also be seen but an increasing ellipticity of the dust cloud was absent. However, in this case, a stretching along the magnetic field direction was not expected due to the much larger forces in the vertical direction (which are responsible for the two-dimensionality of the particle trap). But again, a plasma-related effect could be excluded.

3.3. The influence of the illumination laser

In our experiments, we have observed that the dynamical and structural behavior of the dust system changes strongly when the laser illumination is switched on. This behavior is illustrated in figure 7, to allow study of the ellipticity. This experiment in figure 7(a) was performed with the red laser at 664 nm and approximately 14 mW output power. The laser and magnetic field

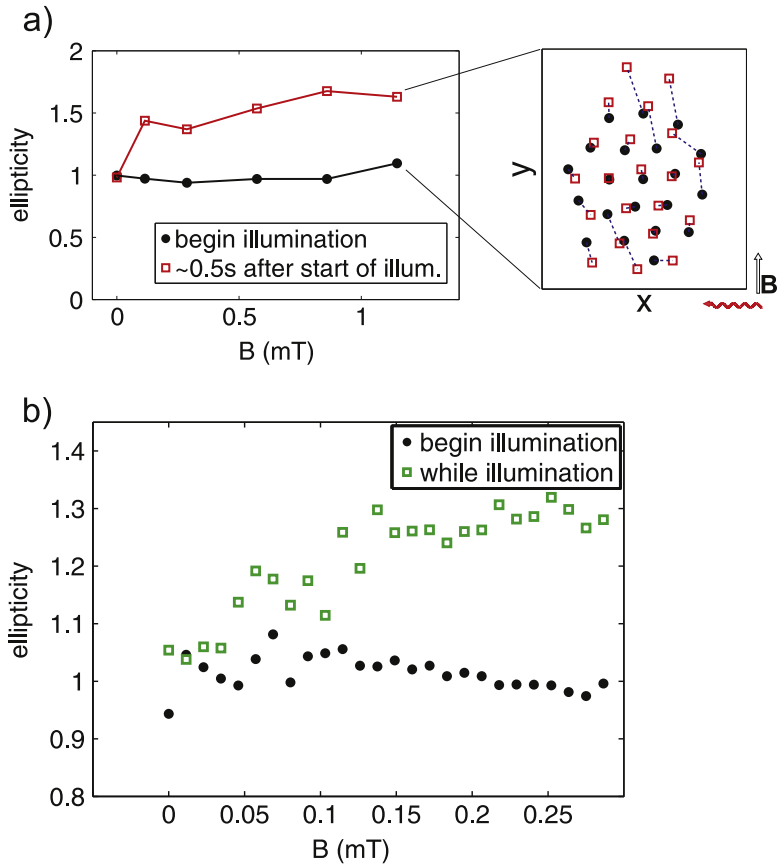

Figure 7. Dependence of the ellipticity on the magnetic field strength and laser light power. In (b) the ellipticity is studied with higher resolution in the magnetic field strength. Note that parts (a) and (b) show different experiments. The inset of figure 7(a) shows mean particle positions for the two cases 'laser off' and 'laser on'.

directions were perpendicular to each other. The experiments in figure 7(b) were performed with the green laser illumination at 28 mW. In both cases the gas pressure was 10 Pa. In figure 7 the ellipticity is plotted as a function of magnetic field strength, this time, however, for the two cases where the laser light is just turned on (black full circles) and where the cluster has already been illuminated for half a second. One can see that the occurrence of the stretching depends on both the magnetic field strength and the existence of the laser illumination. Figure 7(b) gives a more detailed view of the ellipticity at low magnetic fields. One can see from the video images that the cluster is in a hexagonally ordered crystalline state and the ellipticity is close to unity at the very beginning of the laser illumination. Due to the illumination, the particles gain a much higher kinetic temperature and the cluster starts to lose its order when a low magnetic field is present. It is often clearly seen that some particles of the ensemble start a much faster movement or rotation than the others when $B = 0$ and the laser is turned on. Then the whole cluster starts to melt by Coulomb collisions in such a way that an ordered structure is not observed. This happens on a time scale of $\lesssim$1 s. With somewhat larger external magnetic field and 'laser on', the particles mainly perform oscillations around their equilibrium positions and the cluster keeps a relatively low temperature but stretches along the field; compare figure 4. In conclusion, we can say that the temperature of the dust cluster and the stretching along the magnetic field

Table 1. The dust particle charge as a function of the field B remains essentially constant.

B/mT	0	0.11	0.23	0.34	0.46	0.57	0.69	0.8	0.92
Z/-e	8500	8500	8500	8600	8600	8500	8500	8400	8200

axis are coactions of the illumination laser and magnetic field. It is also found that the occurrence of the stretching was unaffected by the direction of the laser beam, and an increase in laser power means an increase in ellipticity. As mentioned before, MF particle systems do not show this behavior. So, a pure plasma effect cannot be held responsible for this. By increasing the number of particles (for a better statistic) forming a two-dimensional dust cloud, it could be demonstrated that this stretching tends to be symmetric around the original center of mass position. This means that on average, equal numbers of particles move in the field direction as well as opposite to the field direction, yielding an ellipticity greater than unity. The total average displacement from the center of mass position is essentially zero. For this, compare the inset of figure 7(a). There, the particle positions corresponding to the case of maximum magnetic field are plotted and the dashed lines mark the displacements of each particle when the illumination laser is switched on.

3.4. Charge measurement

In order to check whether changes in plasma density (amount and distribution) that might occur due to the external magnetic field affect the electrical charge of the dust particles, the normal modes of the cluster were measured. In general, a normal mode of an oscillating finite system is a pattern of motion where all parts of the system oscillate harmonically at the same frequency. Every normal mode is characterized by its shape, i.e. distribution of amplitudes and directions in the particle motion. The full dynamics of the system is contained in a superposition of all normal modes. The normal modes are obtained as the solution of the eigenvalue problem of the dynamical matrix A, which contains the second derivatives of the total potential energy (see equation (1)). To obtain the normal modes from the experiment, the spectral power density of the particle motion along the different modes is calculated from the particle trajectories [24]. The absolute values of the mode frequencies scale with the particle charge. Hence, from the measured mode frequencies, the dust charge is extracted. To use this method we prepared our dust cluster in such a way that the cluster did not melt or stretch under the influence of the illumination laser and the magnetic field. In order to do this, the laser pulses were made very short and weak (pulse width = 0.01 s and output power = 2 mW at a repetition rate of 25 Hz). This measurement was performed at a neutral gas pressure of 10 Pa and the 9 μm superparamagnetic particles were used here. The particle charges are given in table 1 for different field strengths. The dust charge is found to be nearly constant in this regime of magnetic field strengths and hence charge variations cannot be held responsible for the experimental findings described before in section 3.2. The values obtained, of a few thousand elementary charges, are in good agreement with other experiments [24] and analytical models including ion–neutral charge-exchange collisions [25].

3.5. Discussion

It was shown that the stretching of the dust cluster occurred when both the magnetic field and the illumination laser were turned on. Giving an adequate explanation for the combined influence of laser and magnetic field is difficult. At least some laser-induced mechanisms disturbing the particles can be ruled out. The laser power density was low enough to ensure that the radiation pressure is negligible. Nosenko *et al* reported a laser-induced rocket force on microparticles to explain random-direction particle accelerations; see [26]. The authors argue that the rocket force arises due to a local sputtering or evaporation of particle material at the surface. But, in our experiment, we use laser power densities to illuminate the particles that are at least seven orders of magnitude smaller than those of [26]. Hence, laser evaporation seems to be unlikely, in our case, to explain the observed forces. Due to the low laser power, photophoresis is also expected to have no significant influence. A de-charging of the particles due to photo-detachment which would lead to a weaker coupling is not expected. Due to the vertical force balance, a reduced charge would lead to a decrease in levitation height which has not been observed.

A stretching of the dust cloud could occur due to interaction of an electric dipole with the charge of the other particles. Electric dipoles can result from inhomogeneous charge distributions on the particles. These charge inhomogeneities might be supported by alignment of the magnetic movement of the particles in the magnetic field. The local magnetic field distribution around the particles might influence the electron flow to the particle and hence result in an inhomogeneous charge distribution. However, simple MD calculations show that the electric dipole moments that are required for seeing the observed influence on the particle structure have to be of the order of 10^{-19}Asm. For a 5 μm radius particle (charge separation 10 μm), a dipole charge of about 10^5 elementary charges would be required, which is much too large to be reasonable.

It was mentioned before that the magnetic dipole–dipole interaction is very weak compared to the Yukawa interaction. For the case where two particles are arranged in a line along their magnetic moments, the magnetic dipole–dipole interaction force has its largest absolute value and can be written as

$$F_{magn} = -\frac{\mu_0}{4\pi}\frac{6M^2}{r_{ij}^4}. \tag{8}$$

Using the values obtained (for the 9 μm particles) for the magnetic moment, $M = 7.7 \times 10^{-12}$ A m^{-2}, and the interparticle distance, $r_{ij} = 800$ μm, yields a force that is about four orders of magnitude smaller than the electrical force between the particles. Thus, magnetic dipole–dipole interaction cannot lead to a structural change of the particle cluster. Even if the particle magnetic moments were to be saturated ($M = 1.4 \times 10^{-11}$ A m^2), the magnetic force would still be smaller by a factor of $\approx$100. We should also comment on the spinning of dust grains which also causes magnetic moments. The possible rotation frequencies given in the literature are of the order of up to $f = 10^6$ Hz [27–30]. With the typical dust charges, this leads to magnetic moments that are several orders of magnitude smaller than the maximum magnetic moments reached in this work caused by an external B-field. So, the spin magnetization of dust particles is negligible.

If plasma modifications induced by the external magnetic field were to cause the observed stretching and temperature decrease, the MF particles would also be influenced. But those are found to be unaffected.

Such paramagnetic particles have also been widely used in (electrically conducting) colloidal suspensions with magnetic fields; see e.g. [31]. Also there, only flows perpendicular to the magnetic field are observed; however forces along a homogeneous field have not been described. This supports our interpretation that we have a more complicated interaction in our dusty plasma experiments.

4. Summary

In this work, paramagnetic dust particles trapped in an argon rf discharge with a weak external magnetic field were studied. We have seen that these systems behave very differently as compared to clusters consisting of MF particles. Differences from MF systems include e.g. the stretching along the axis of the magnetic field, and the large temperatures at $B \simeq 0$, as well as the cooling down of the particle systems with increasing magnetic field. It was shown that this behavior is caused by a coaction of the magnetic field and illumination laser. Turning on the laser light caused an increase in cluster temperature and disorder, while an increase in magnetic field strength decreased the temperature again. Ellipticity of the dust clusters arose when both the magnetic field and the laser illumination were turned on. Both illumination lasers yielded qualitatively the same experimental findings. From the normal mode analysis, we have seen that the dust charge remains constant in this magnetic field regime; thus it cannot contribute to this behavior. Plasma effects can be ruled out from the comparison with MF particles.

The single-particle movement and the displacement of the whole cluster are well understood and can be explained by a superposition of a $\nabla\vec{B}$-force and the ambipolar $\vec{E} \times \vec{B}$-drift. The displacement perpendicular to the magnetic field axis explained by the ambipolar $\vec{E} \times \vec{B}$-drift is a plasma effect.

Acknowledgments

This work was supported by the Deutsche Forschungsgemeinschaft via SFB-TR24 Grant A3.

References

[1] Ikezi H 1986 Coulomb solid of small particles in plasmas *Phys. Fluids* **29** 1764–6
[2] Thomas H, Morfill G E, Demmel V, Goree J, Feuerbacher B and Möhlmann D 1994 Plasma crystal: Coulomb crystallization in a dusty plasma *Phys. Rev. Lett.* **73** 652–5
[3] Chu J H and I L 1994 Direct observation of coulomb crystals and liquids in strongly coupled rf dusty plasmas *Phys. Rev. Lett.* **72** 4009–12
[4] Chu J H and I L 1994 Coulomb lattice in a weakly ionized colloidal plasma *Physica A* **205** 183–90
[5] Melzer A, Trottenberg T and Piel A 1994 Experimental determination of the charge on dust particles forming coulomb lattices *Phys. Lett.* A **191** 301–8
[6] Trottenberg T, Melzer A and Piel A 1995 Measurement of the electric charge on particulates forming coulomb crystals in the sheath of a radiofrequency plasma *Plasma Sources Sci. Technol.* **4** 450

[7] Arp O, Block D, Piel A and Melzer A 2004 Dust coulomb balls: Three-dimensional plasma crystals *Phys. Rev. Lett.* **93** 165004
[8] Kushner M J 2003 Modeling of magnetically enhanced capacitively coupled plasma sources: Ar discharges *J. Appl. Phys.* **94** 1436–47
[9] Kelly P J and Arnell R D 2000 Magnetron sputtering: a review of recent developments and applications *Vacuum* **56** 159–72
[10] Turner M M, Hutchinson D A W, Doyle R A and Hopkins M B 1996 Heating mode transition induced by a magnetic field in a capacitive rf discharge *Phys. Rev. Lett.* **76** 2069–72
[11] Avtaeva S V, Mamytbekov M Z and Otorbaev D K 1997 Diagnostics of magnetically enhanced rf discharges in methane argon and methane—argon mixtures *J. Phys. D: Appl. Phys.* **30** 3000
[12] Barnat E V, Miller P A and Paterson A M 2008 Rf discharge under the influence of a transverse magnetic field *Plasma Sources Sci. Technol.* **17** 045005
[13] Samsonov D, Zhdanov S, Morfill G and Steinberg V 2003 Levitation and agglomeration of magnetic grains in a complex plasma with magnetic field *New J. Phys.* **5** 24
[14] Hartmann P, Rosenberg M, Kalman G J and Donkó Z 2011 Ground-state structures of superparamagnetic two-dimensional dusty plasma crystals *Phys. Rev.* E **84** 016409
[15] Feldmann J D, Kalman G J, Hartmann P and Rosenberg M 2008 Ground state of magnetic dipoles on a two-dimensional lattice: Structural phases in complex plasmas *Phys. Rev. Lett.* **100** 085001
[16] Konopka U, Samsonov D, Ivlev A V, Goree J, Steinberg V and Morfill G E 2000 Rigid and differential plasma crystal rotation induced by magnetic fields *Phys. Rev.* E **61** 1890–8
[17] Matyash K, Fröhlich M, Kersten H, Thieme G, Schneider R, Hannemann M and Hippler R 2004 Rotating dust ring in an RF discharge coupled with a dc-magnetron sputter source. Experiment and simulation *J. Phys. D: Appl. Phys.* **37** 2703–8
[18] Carstensen J, Greiner F, Hou L J, Maurer H and Piel A 2009 Effect of neutral gas motion on the rotation of dust clusters in an axial magnetic field *Phys. Plasmas* **16** 013702
[19] D'yachkov L G, Petrov O F and Fortov V E 2009 Dusty Plasma Structures in Magnetic DC Discharges *Contrib. Plasma Phys.* **49** 134–47
[20] Microparticles GmbH www.microparticles.de
[21] Maemura Y, Yang S C and Fujiyama H 1998 Transport of negatively charged particles by e A–b drift in silane plasmas *Surf. Coat. Technol.* **98** 1351–8
[22] Vaulina O S, Khrapak S A, Nefedov A P and Petrov O F 1999 Charge-fluctuation-induced heating of dust particles in a plasma *Phys. Rev.* E **60** 5959–64
[23] Quinn R A and Goree J 2000 Single-particle langevin model of particle temperature in dusty plasmas *Phys. Rev.* E **61** 3033–41
[24] Melzer A 2003 Mode spectra of thermally excited two-dimensional dust coulomb clusters *Phys. Rev.* E **67** 016411
[25] Khrapak S A *et al* 2005 Particle charge in the bulk of gas discharges *Phys. Rev.* E **72** 016406
[26] Nosenko V, Ivlev A V and Morfill G E 2010 Laser-induced rocket force on a microparticle in a complex (dusty) plasma *Phys. Plasmas* **17** 123705
[27] Krasheninnikov S I 2006 On dust spin up in uniform magnetized plasma *Phys. Plasmas* **13** 114502
[28] Krasheninnikov S I, Shevchenko V I and Shukla P K 2007 Spinning of a charged dust particle in a magnetized plasma *Phys. Lett.* A **361** 133–5
[29] Hutchinson I H 2004 Spin stability of asymmetrically charged plasma dust *New J. Phys.* **6** 43–9
[30] Tsytovich V N, Sato N and Morfill G E 2003 Note on the charging and spinning of dust particles in complex plasmas in a strong magnetic field *New J. Phys.* **5** 43–51
[31] Nguyen N T 2012 Micro-magnetofluidics: interactions between magnetism and fluid flow on the microscale *Microfluid Nanofluid* **12** 1–16